Renewable Energy 78 (2015) 105–113

Contents lists available at ScienceDirect

Renewable Energy

journal homepage: www.elsevier.com/locate/renene

A three diode model for industrial solar cells and estimation of solar cell parameters using PSO algorithm

Vandana Khanna [a], B.K. Das [a, *], Dinesh Bisht [b], Vandana [c], P.K. Singh [c]

[a] ITM University, Gurgaon 122017, India
[b] JIIT University, Noida 201307, India
[c] CSIR-National Physical Laboratory (Network of Institutes for Solar Energy), New Delhi 110012 India

ARTICLE INFO

Article history:
Received 18 April 2014
Accepted 29 December 2014
Available online

Keywords:
Solar cell
PSO algorithm
Parameter estimation
Two-diode model
Three-diode model

ABSTRACT

A new lumped-parameter equivalent circuit model using three-diodes is presented in this work for large area (~154.8 cm^2) industrial silicon solar cells. The estimation of values of ideality factors n_1 (>1) and n_2 (>2) using a Particle Swarm Optimization (PSO) algorithm for the two-diode model of the industrial samples has been found not to be in conformity with the theoretical values ($n_1 = 1$ and $n_2 = 2$ in the literature). The two diodes of the two-diode model are not able to define the different current components of the solar cells clearly. A model with three-diodes has been proposed to better explain the experimental data. In the proposed model, we considered the series resistance, R_s, of the solar cell to vary with the current flowing through the solar cell device. All the parameters of the proposed model have been estimated using a PSO algorithm and they were compared with the parameters of the two-diode model. The new model has been found to be a better model to define clearly the different current components of the large size industrial silicon solar cells.

1. Introduction

Modeling of a solar cell is required to predict the behaviour of a real solar cell under various environmental conditions and thereafter to generate its current–voltage (I–V) and power-voltage (P–V) characteristic curves. The common approach is to utilize the electrical equivalent circuit, which is primarily based on a light generated current source connected in parallel to a p–n junction diode. Many models have been proposed for the simulation of a single solar cell or for a complete photovoltaic (PV) system at various solar intensities and temperature conditions [1–5]. Different models have also been used to study the shading effect on PV systems [6–8]. Two most commonly used equivalent circuit models of the solar cell in the literature are one-diode and two-diode models [1–8].

1.1. One-diode and two-diode models

An ideal solar cell is represented by a light generated current source, I_{ph}, where I_{ph} is proportional to the solar radiation falling on it. Practical light generated current behaviour deviates from the ideal behaviour due to optical and electrical losses inside the solar cell. In the one-diode model, one diode is connected in parallel to a light generated current source as shown in Fig. 1(a). Diode current, I_d, represents the current due to diffusion and recombination in the Quasi Neutral Regions (QNRs) of the emitter and bulk regions of the P–N junction. The series resistance, R_s, represents the resistance in the path of the current, due to contact resistances and resistance in the emitter and bulk regions. Shunt resistance, R_{sh}, represents the current leakage across the P–N junction of the solar cell and so it is connected in parallel to the diode in the equivalent circuit model. On the other hand, the two-diode model shown in Fig. 1(b) considers two-diodes connected in parallel to the current source. The current through the first diode, I_{d1}, is the current component, which is the same as I_d in the one-diode model. The current due to recombination in the Space Charge Regions (SCRs) is also considered in the two-diode model and is represented by the diode current, I_{d2} through a second diode. Series resistance, R_s, and shunt resistance, R_{sh}, are the same resistance components as defined for the one-diode model.

The load current (I) and the load voltage (V) are related through Eqs. (1a) and (2a) for the one-diode and the two-diode models respectively.

* Corresponding author.
E-mail address: bkdas45@yahoo.co.uk (B.K. Das).

http://dx.doi.org/10.1016/j.renene.2014.12.072
0960-1481/

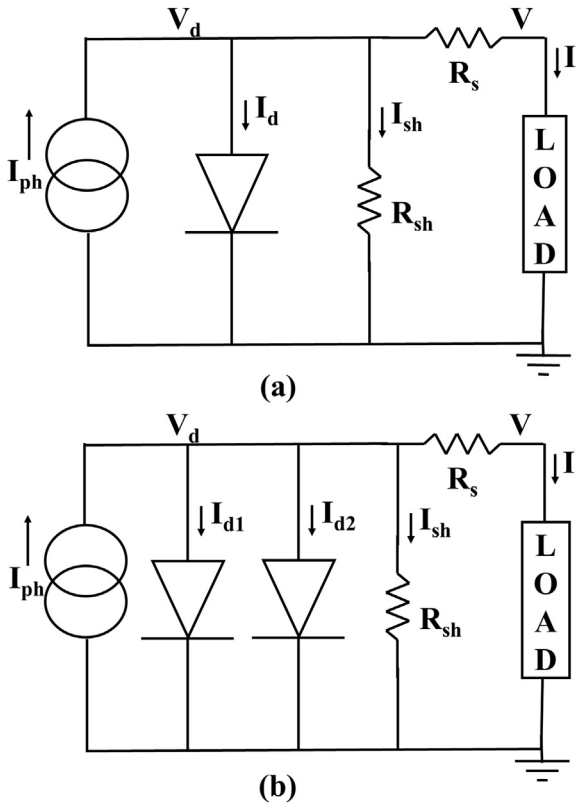

Fig. 1. (a) One-diode model of a solar cell (b) Two-diode model of a solar cell.

$$I = I_{ph} - I_0\left\{exp\left[\frac{q(V+IR_S)}{nkT}\right] - 1\right\} - \frac{V+IR_S}{R_{sh}} = I(V, I, parameters1) \tag{1a}$$

$$where\ parameters1 = \left\{I_{ph},\ I_0,\ n,\ R_S,\ R_{sh}\right\} \tag{1b}$$

$$I = I_{ph} - I_{01}\left\{exp\left[\frac{q(V+IR_S)}{n_1kT}\right] - 1\right\} - I_{02}\left\{exp\left[\frac{q(V+IR_S)}{n_2kT}\right] - 1\right\} - \frac{V+IR_S}{R_{sh}} = I(V, I, parameters2) \tag{2a}$$

$$where\ parameters2 = \left\{I_{ph},\ I_{01}, n_1, I_{02}\ , n_2,\ R_S, R_{sh}\right\} \tag{2b}$$

For one-diode model, the value of ideality factor, n, is between 1 and 2. For two-diode model, two ideality factors, n_1 and n_2 should be 1 and 2 respectively.

The number of parameters as given in Eq. (1b) for modeling in case of the one-diode model is five. These parameters are light generated current, I_{ph}, diode parameters: reverse saturation current, I_0, and ideality factor, n, series resistance, R_s, and shunt resistance, R_{sh}. In the two-diode model, the number of parameters becomes seven as given in Eq. (2b). The parameters are the reverse saturation currents I_{01} and I_{02} and ideality factors n_1 and n_2 for the two diodes, along with other parameters - I_{ph}, R_s and R_{sh}. Estimation of all parameters of a solar cell model is required for modeling the performance of any photovoltaic system. Many analytical and numerical methods [9–14] have been suggested in the literature to estimate some or all parameters of the one-diode model or the two-diode model from measured I–V characteristics. Heuristic methods such as genetic algorithms, pattern search algorithm, differential evolution and particle swarm optimization have been suggested by others [15–26] for the same purpose. Heuristic methods have shown better precision and computational efficiency for estimation of solar cell parameters as compared to analytical and numerical methods. Recently, a swarm intelligence based method called Particle Swarm Optimization (PSO) has been successfully applied to various fields of power system. Phuangpornpitak et al. [19] have presented a survey on the application of PSO in solving optimization problems in electric power systems. Kongnam and Nuchprayoon [20] have applied PSO to a wind energy control problem. PSO algorithm has been used to solve for optimum rotor speed under fixed-speed operation and optimum tip-speed ratio under variable-speed operation. Qin and Kimball [21] presented an approach to extract parameters of a PV cell using PSO. PSO was applied only on single diode model and some parameters were predicted beforehand. Only n, R_s and R_{sh} were estimated using PSO. Sandrolini et al. [22] used a PSO algorithm for the extraction of the double-diode model parameters of photovoltaic (PV) modules. Authors used PSO algorithm to fit the calculated current–voltage characteristic of a PV module to the experimental one.

In this paper, a new lumped-parameter equivalent circuit model using three diodes, has been proposed for large area crystalline silicon solar cells. In addition, in the proposed model, the parameter, R_s has been considered to vary linearly with the load current through the device and thus the variation of R_s with the load current has been studied on the same large area solar cell samples in this work. The aim of this work is to suggest a better model for the bigger size industrial solar cells and to estimate the parameters of the model by fitting the calculated I–V curves to the measured I–V curves, through an iterative process using the PSO algorithm.

This paper is organized as follows. Section 2 discusses the theory of the proposed model followed by an overview of the PSO algorithm. Section 3 describes the experimental methods used for the fabrication of the solar cell samples and measurement of the current–voltage characteristics. The procedure used for parameter extraction is discussed in Section 4. Results are discussed in Section 5. The comparison of two models, existing and new, is highlighted in Section 6 and finally the paper is concluded in Section 7.

2. Theory

2.1. Proposed model: three-diode model with variable R_s

For the two-diode model, the ideal values of n_1 and n_2 would be 1 and 2 respectively; but for industrial samples of size as big as about 154.8 cm^2 and efficiency about 16%, n_1 was estimated between 1 and 1.5 and n_2 was estimated between 2 and 5. These values indicated that the two diodes were not sufficient to represent the different current components of the experimental solar cells clearly.

In this work, a three-diode model has been proposed, as illustrated in Fig. 2. In the model, the first diode would contribute the diode current (I_{d1}) due to diffusion and recombination in the quasi neutral regions (QNRs) of the emitter and bulk regions with $n_1 = 1$, and the second diode would contribute the diode current (I_{d2}) due to recombination in the space charge region (SCR) with $n_2 = 2$. The purpose of adding a third diode in parallel to the two diodes is to consider contribution of the diode current component (I_{d3}), due to recombination in the defect regions, grain sites, etc. The ideality factor, n_3, of the third diode is to be estimated along with other parameters of the model and is predicted to be varying between 2 and 5 depending on the local factors as mentioned in Ref. [27].

SilkeSteingrube et al. [27] proved experimentally and later through simulations that value of the diode ideality factor, n, increases with increase in the defect density, for crystalline Si solar cells. In their work, they found that laser cutting or scratching of the solar cells during fabrication increases the localized defect density. Due to increase in such localized defects, there is an increase in Donor–Acceptor Pairs (DAP). DAPs are most efficient for recombination and hence there is an increase in the recombination rate, leading to higher values of n and value of n can be more than 2 (up to a value of 5), mostly in case of industrially fabricated solar cells. However, in literature [1–8], the theoretical values of ideality factors n_1 and n_2 for two-diode model are 1 and 2 respectively. Nishioka et al. [28] have proposed a three-diode equivalent circuit model for multi-crystalline silicon solar cells of small size (3 mm × 3 mm), to take care of leakage current through periphery; the n values (n_1, n_2 and n_3) for the three diodes have been taken by them as 1, 2 and 2. No method has been mentioned by them for the extraction of parameters in their work. In the present work, we have used PSO algorithm similar to one given by Sandrolini et al [22]. for the extraction of parameters of the existing two-diode model and the proposed new three-diode model.

In this study, series resistance, R_s, was not considered to be constant with load current, I. Rather it has been proposed as a variable parameter, whose value would depend on the variation of the load current. So, to find the variation of R_s with I, R_s was replaced with $R_{so}(1 + KI)$, where I was the load current and K was another parameter, which would be to be determined along with other parameters. Eq. (3a) could thus be used to define the currents through the solar cell using the three-diode model with a variable series resistance.

$$I = I_{ph} - I_{01}\left\{exp\left[\frac{q(V+IR_{so}(1+KI))}{n_1 kT}\right]-1\right\} - I_{02}\left\{exp\left[\frac{q(V+IR_{so}(1+KI))}{n_2 kT}\right]-1\right\} - I_{03}\left\{exp\left[\frac{q(V+IR_{so}(1+KI))}{n_3 kT}\right]-1\right\} - \frac{V+IR_{so}(1+KI)}{R_{sh}} = I\left(V, I, parameters3\right) \quad (3a)$$

$$where\, parameters3 = \left\{I_{ph}, I_{01}, n_1, I_{02}, n_2, I_{03}, n_3, R_{so}, K, R_{sh}\right\} \quad (3b)$$

2.2. Particle swarm optimization (PSO)

Particle Swarm Optimization (PSO) simulates the behaviour of a flock of birds. When a flock of birds searches for food, no bird knows where the food is, but all the birds know the distance to the food. So initially, all the birds move with random velocities and positions, but after a while, based on their own flying experience and the experience of the other birds, all the birds follow the bird that is nearest to the food.

PSO can be applied to any optimization problem; a fitness function (equivalent to the distance from food) is defined that is to be optimized (maximized or minimized). Initially, a number of random solutions of the problem are generated, where each solution is a 'bird' (also called a 'particle') in the search space. All the particles have random positions and velocities. For each iteration, the fitness values corresponding to the fitness function are calculated for each particle and two best fitness values are found, the first is the best fitness value a particle has achieved so far called 'pbest'. The second is the best fitness value obtained so far by any particle in the population, this is called 'gbest'. Each particle's velocity and position are updated by Eq. (4a) and (4b).

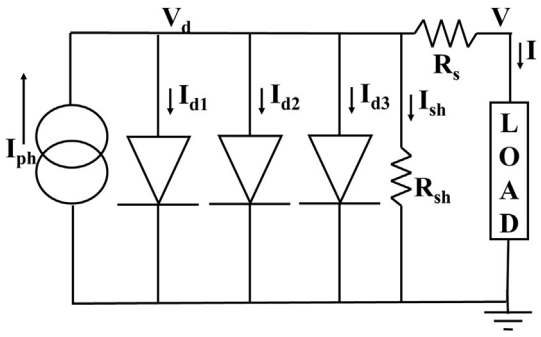

Fig. 2. Proposed Three-diode Model is presented. The first diode would contribute the diode current (I_{d1}) due to diffusion and recombination in the quasi neutral regions (QNRs) of the emitter and bulk regions with $n_1 = 1$, and the second diode would contribute the diode current (I_{d2}) due to recombination in the space charge region (SCR) with $n_2 = 2$. The third diode in parallel to the two diodes would contribution of the diode current component (I_{d3}), due to recombination in the defect regions, grain sites, etc. with $n_3 > 2$.

$$v[\,] = w*v[\,] + c1*rand*(pbest[\,]-x[\,]) + c2*rand*(gbest[\,]-x[\,]) \quad (4a)$$

$$x[\,] = x[\,] + v[\,] \quad (4b)$$

$v[\,]$ is the particle velocity and w is an inertia weight in the range (0, 1) that is generally decreased in value in subsequent iterations. $x[\,]$ is the current particle position. $pbest[\,]$ and $gbest[\,]$ are defined as stated before. *rand* is a random number between (0, 1). $c1$ is a constant called cognitive or local weight. $c2$ is a constant called social or global weight; usually, c1 = c2 = 2. In Eq. (4A), the second term represents a 'cognitive' model, whereas the third term represents a 'social' model. Cognitive model expresses the particle's own experience and social model expresses the collaboration among particles.

Any optimization algorithm requires an exploration-exploitation trade-off that measures the efficiency of the algorithm. A good optimization algorithm optimally balances these contradictory aspects. In PSO, this is done by two ways: inertia weight and velocity clamping [23,24].

Inertia weight w controls the momentum of the particles by assigning weight to the contribution of the particle velocity during the earlier iteration. To ensure convergent behaviour, the value of w is extremely important. Large values of w facilitate exploration with increased diversity and low values promote local exploitation [24]. Dynamically changing value of the inertia weight gives a better trade-off between exploration and exploitation. Optimization usually starts with a large value of w, which decreases over time to a low value. This gives a better initial exploration followed by good local exploitation. In the present work, the initial value of w was taken as 1, which was linearly decreased over iterations to a final value of 0.

Velocity clamping [23,24] is the concept of clamping the velocities of the particles to stay within the boundary constraints. In PSO algorithms, velocities of the particles can easily explode to large values and so positions of particles update to large values beyond the boundaries of the search space. PSO algorithm used in this work has utilized velocity clamping to control the global exploration of particles as per Eq. (4c).

$$v_j[\,] = \begin{Bmatrix} v_j[\,], & if\ v_j[\,] < v_{max,j} \\ v_{max,j}, & otherwise \end{Bmatrix} \quad (4c)$$

$v_{max,j}$ denotes the maximum allowed velocity of a particle in jth dimension in the solution space. The velocity of the particles is adjusted according to Eq. (4c) before position is updated using Eq. (4b). Higher value of $v_{max,j}$ causes exploration and lower value promotes local exploitation. Each jth dimension is assigned a maximum velocity, $v_{max,j}$, proportional to the domain of that dimension. Usually, $v_{max,j}$ value equals a fraction of the domain of each dimension of the search space as given below.

$$v_{max,j} = \delta(x_{max,j} - x_{min,j}) \quad (4d)$$

$$v_{min,j} = \delta(x_{min,j} - x_{max,j}) \quad (4e)$$

where, $x_{max,j}$ and $x_{min,j}$ are the maximum and minimum positions of the particles in jth dimension respectively. For our work, we have taken δ as a constant value of 0.1.

The goal of the particle swarm optimizer is to change each particle's velocity and position iteratively to achieve the particle's best results and overall best solution. The flowchart of PSO algorithm is shown in Fig. 3. In the present work, PSO algorithm has been applied to the problem of estimation of all parameters of the two-diode solar cell model and the proposed 3-diode model, which was done by fitting the calculated I–V curves to the measured I–V curves for different solar cell samples. The fitness function to be optimized was taken as the average absolute value of the difference between $I_{calculated}$ and $I_{measured}$ for all measured points in the I–V curve at each iteration, which needed to be minimized to get the best estimation of parameters. The particles were the randomly generated sets of unknown parameters, with random velocities and positions. Through the iterative process of PSO, the position and velocities of the particles were updated, until either a relatively unchanging condition of the fitness function was reached or a specified number of iterations were done.

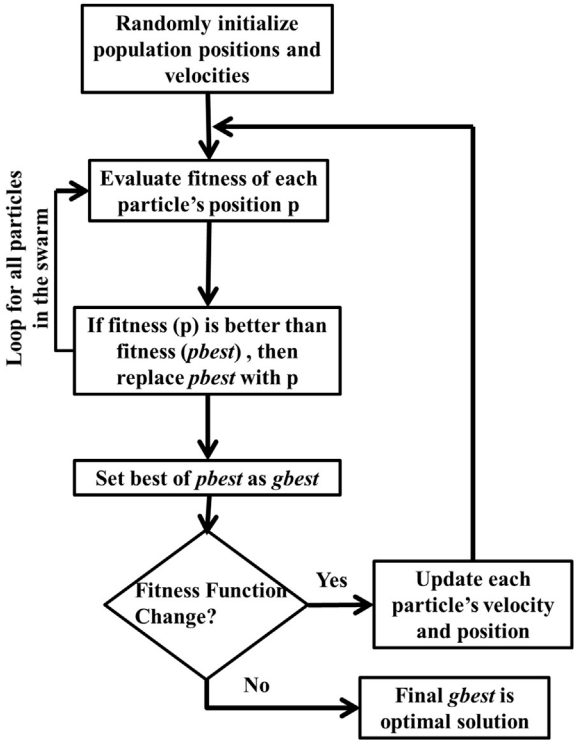

Fig. 3. Flowchart of the PSO Algorithm used is presented. Fitness function is estimated after each iteration and the iteration terminates if Fitness function does not change significantly or after a certain number of iterations.

3. Experimental methods

In the present study, an I–V measurement system (M/s Newport Corporation, Model: J80036) with adjustable 3 bus bar nest assembly (26 pin each) was used. It consisted of a solar simulator, electrical measurement system interfaced with a LabVIEW based software. The solar simulator (Model: Oriel Sol3A, M/s Oriel Instrument USA, meeting IEC 60904-9 (2007); ASTM E 927-05 (2005) and JIS C 8912-1998 standards) used a CW Xenon arc lamp (1600 W and had an output beam sizes of 20 × 20 cm^2) with an AM1.5G filter meeting the performance in terms of spectral match to the solar spectrum, spatial non-uniformity of irradiance and temporal instability of irradiance. The system had a temperature controlled vacuum positioning cell chuck held at 25 °C with a temperature accuracy ±0.25 °C. To vary light output from 0.1 to 1.0 sun, an integrated variable attenuator was provided. The rating of the current measurement facility was up to 10 amp. The measurement accuracies of voltage and current were 0.002% (0.00001 mV) and 0.002% (0.00001 mA) respectively. It had a calibrated reference cell that could be used for tuning the solar simulator power level to the test conditions. The LabVIEW based software calculated parameters such as short circuit current (I_{sc}), short circuit current density (J_{sc}), open circuit voltage (V_{oc}), fill factor (ff), maximum output power (P_{max}), maximum output voltage (V_{max}), maximum output current (I_{max}), cell efficiency (η), shunt resistance (R_{sh}) and series resistance (R_s).

The n^+-p-p^+ structure based silicon solar cells (154.8 cm^2) used in this study were from production line of an Indian PV industry. Each cell was made on a p-type boron doped CZ single-crystalline silicon wafer (typical minority carrier lifetime ~10 μs) using $POCl_3$ diffusion to make the p^+–n diode, back aluminium diffusion to have a p^+ layer and electrical contacts to extract the electrical current by the screen printing technology. The cell incorporated several optical engineering elements such as random textured surface (in alkaline solution) to reduce reflectance and removal of damage caused by the wire-sawing process, and a back surface field by aluminium diffusion to reduce recombination losses. A silicon nitride layer was also used as an antireflective coating to further reduce the reflectivity and to passivate the front surface. These solar cells had conversion efficiency (AM1.5G) in the range of 16–18%.

4. Procedure

Particle Swarm Optimization technique as described in Section 2.2 was applied to fit the calculated I–V curves for the two-diode model (Eq. (2a)) and for proposed three-diode model (Eq. (3a)) to the measured I–V curves of the solar cell samples mentioned in Section 3.

4.1. Models

Following two models were investigated in this work.

a) Two-diode model with Fixed R_s: I_{ph} was assumed to be fixed and equal to I_{sc} (short-circuit current). The parameters to be estimated were I_{01}, n_1, I_{02}, n_2, R_s and R_{sh} (Eq. (2b)).
b) Three-diode model with Variable R_s: Out of 10 parameters of Eq. (3b), I_{ph} was assumed to be fixed and equal to I_{sc}, n_1 and n_2 were assumed to be fixed as 1 and 2 respectively. Therefore, the parameters to be estimated were: I_{01}, I_{02}, I_{03}, n_3, R_{so}, K and R_{sh}.

Table 1
The values of estimated parameters in multiple runs with same set-up for PSO for sample V6 using the two-diode model (I_{sc} = 5.5535A for V6 Sample).

Runs	I_{01} (nA)	n_1	I_{02} (μA)	n_2	R_s (mΩ)	R_{sh} (Ω)	MAE (A)
1	5.94	1.209	22.1	2.677	8.86	20.166	0.00598
2	4.77	1.198	9.55	2.376	8.88	20.383	0.00594
3	7.36	1.222	10.4	2.467	8.77	20.260	0.00590
4	4.77	1.197	11.9	2.438	8.88	20.554	0.00596
5	7.35	1.221	30.6	2.852	8.82	20.395	0.00596
6	4.86	1.198	9.89	2.393	8.90	21.744	0.00594
7	7.37	1.222	16.1	2.602	8.79	21.307	0.00589
8	5.19	1.201	22.8	2.667	8.90	20.647	0.00600
9	8.71	1.232	11.0	2.513	8.70	21.095	0.00590
10	5.41	1.204	9.61	2.400	8.86	19.655	0.00595
11	5.06	1.200	20.2	2.609	8.89	21.529	0.00596
Standard Deviation	1.38	0.0123	7.11	0.1501	0.064	0.6396	3.48E-05

The values of short-circuit current (I_{sc}) were taken from the measured data for different samples.

4.2. Matlab coding

Matlab coding was used for the PSO algorithm, which worked on optimization of an objective/fitness function through iterations. During each iteration, the root of the functions of Eq. (5a) or 5b was calculated at each point in the I–V curve using the *Newton Raphson method* for arriving at $I_{calculated}$ at any voltage for a solar cell.

$$\text{For two} - \text{diode model}: \; I_{calculated} - I(V, I_{calculated}, \; parameters2) = 0 \tag{5a}$$

$$\text{For proposed three} - \text{diode model}: I_{calculated} - I(V, I_{calculated}, \; parameters3) = 0 \tag{5b}$$

Fitness Function: The fitness function, which is a measure of error during PSO optimization, was defined as the mean of the absolute errors at each point in the I–V curve.

Mean Absolute Error (MAE) and Individual Absolute Error (IAE) were defined as follows:

$$MAE = \frac{\sum_{i=1}^{n} |(I_{calculated} - I_{measured})|}{n} = \frac{\sum_{i=1}^{n} IAE}{n} \tag{6}$$

where n was the number of points of measurement, which were ~ 2500 in this work.

Ideally, MAE should be zero, if calculated curve matches 100% with the measured curve. Practically, PSO algorithm reduced MAE up to third decimal place after 500 iterations and the calculated and measured curves gave a good fit.

4.3. PSO a random and heuristic method

In PSO algorithm, an optimized solution is usually achieved in a number of iterations using a random approach. Repeated PSO runs (each run = 500 iterations) for the same set of experimental I–V data do not give recurrent results, mainly because of the random nature of the PSO algorithm. Multiple runs (10–12) were carried out for each solar cell sample to check the variation in results. Results of different runs for one sample V6, are shown in Table 1 for the two-diode model. From the values of standard deviation of different estimated parameters, we could interpret that though PSO is a random algorithm, the results achieved in multiple runs were.

5. Results & discussion

5.1. 2-Diode model

Comparison of calculated and measured I–V plots for 12 industrial samples was carried out for the two-diode model using the PSO algorithm. The parameters of the model were estimated by fitting of the calculated I–V curve to the measured I–V curve with the least achievable MAE. The calculated and measured I–V curves for two solar cells have been shown in Fig. 4, illustrating the good match obtained between the two curves. For Sample V1, the MAE obtained was 0.00626A, which in percentage term was 0.11% of I_{sc}. Similarly, for sample V2, the MAE obtained was 0.00603A, which was 0.107% of I_{sc}. Out of 12 samples, the best and worst MAE values achieved through PSO algorithm were 0.092% and 0.15% of I_{sc} respectively.

Fig. 5(a) shows plots of $I_{measured}$, $I_{calculated}$ and Individual Absolute Error (IAE) vs. output voltage for sample V1. Out of the twelve solar cells studied, I–V and IAE plots for sample V3 (with best MAE) and for sample V8 (with worst MAE) are shown in Fig. 5(b) and (c) respectively. It can be observed that the values of IAE were comparatively small near the maximum power-points in all the cases. Newton Raphson method had convergence issues mainly

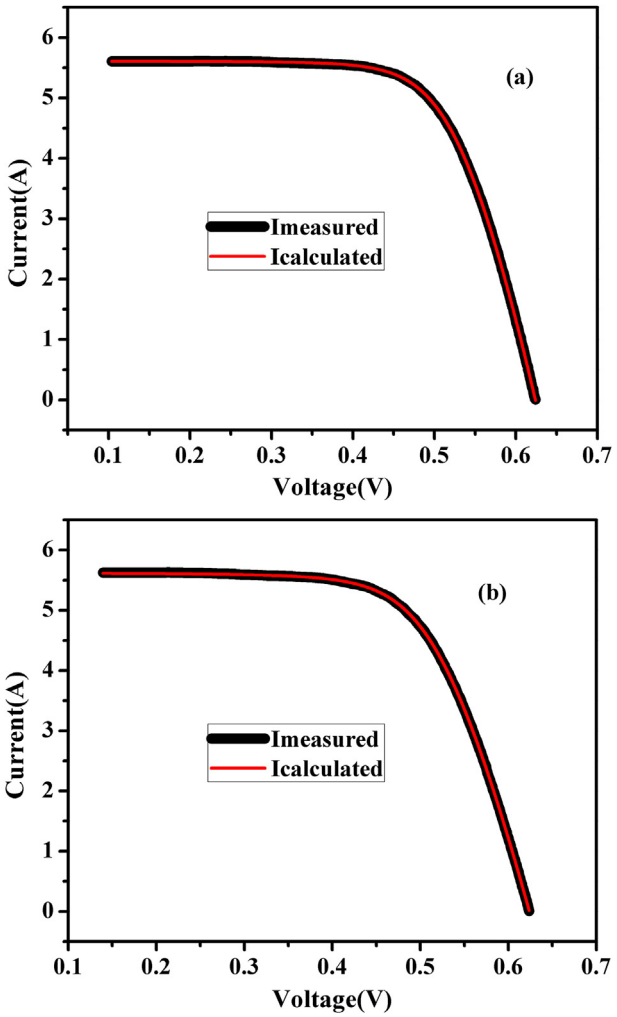

Fig. 4. Measured and calculated I–V characteristics for Sample V1 (a) and Sample V2 (b). There was good match between the measured and calculated I–V characteristics for the two samples.

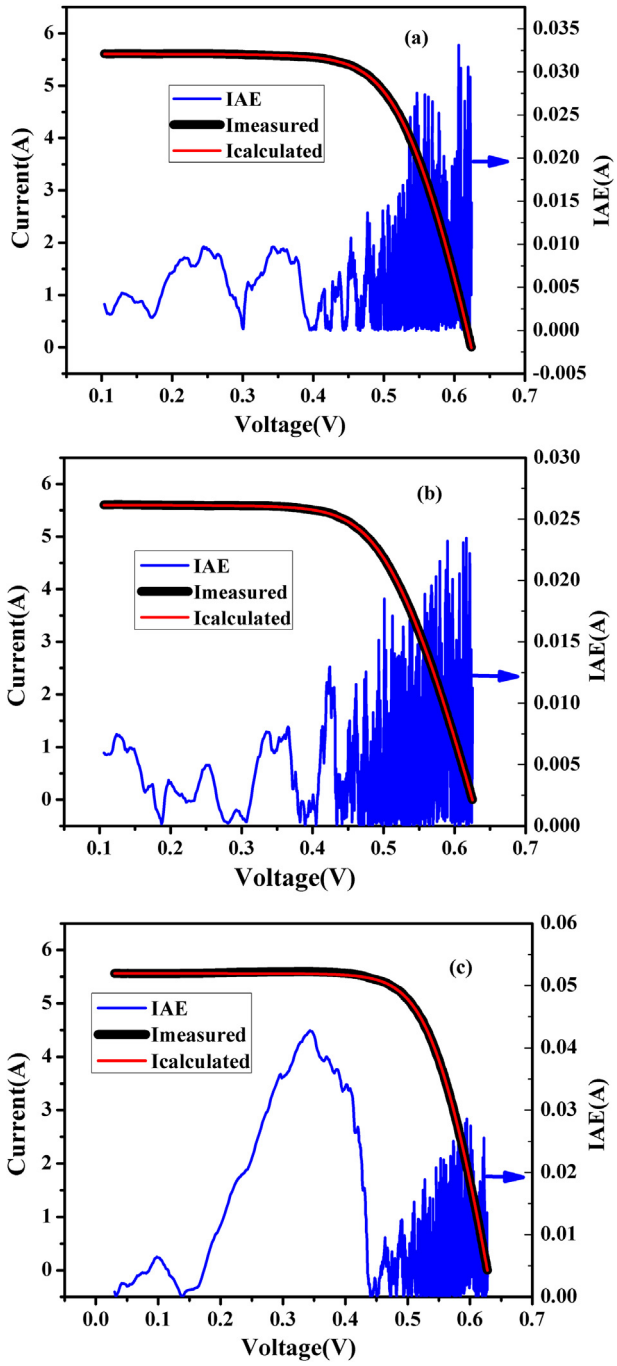

Fig. 5. I–V (measured and calculated) characteristics and Individual Absolute Error (IAE) for (a) Sample V1 (MAE = 0.11%), (b) Sample V3 (best MAE = 0.092%) and (c) Sample V8 (worst MAE = 0.15%). Wide variation in IAE near V_{oc} was due to convergence issue of the Newton Raphson method there.

near the open-circuit voltage (V_{oc}), and hence the IAE values were high near V_{oc}.

The estimated parameters of 12 industrial samples of solar cells using PSO algorithm for the two-diode model are tabulated in Table 2. The values of parameters were considered from the PSO run with least MAE out of 10–12 runs. The values of n_1 for all samples were around 1.2 and values of n_2 for all samples were between 2.5 and 3.0. Rs varied from 8 mΩ to 15 mΩ, for different samples and R_{sh} for different samples varied over a wider range from 9 Ω to 105 Ω. I_{01} and I_{02} for all samples were almost in the same range (within an order of magnitude). MAE values were less than 0.001 A in all samples, which meant a very good fit of the calculated I–V characteristics to the measured I–V characteristics for all the solar cells. It can be seen that $n_1 > 1$ and $n_2 > 2$, though theoretically one should get $n_1 = 1$ and $n_2 = 2$.

Table 2
Estimated parameters using PSO algorithm for two-diode model.

Samples	I_{01} (nA)	n_1	I_{02} (μA)	n_2	R_s (mΩ)	R_{sh} (Ω)	MAE (A)
V1	6.449	1.216	36.2	2.727	11.67	63.46	0.00626
V2	4.311	1.195	63.32	2.794	13.29	16.183	0.00604
V3	8.399	1.233	15.29	2.57	15.15	33.704	0.00516
V4	11.15	1.25	18.78	2.669	11.86	9.6404	0.00602
V5	7.367	1.222	16.14	2.602	8.79	21.307	0.00589
V6	2.255	1.158	36.31	2.853	12.42	13.985	0.00648
V7	4.445	1.195	10.96	2.493	11.13	15.187	0.00552
V8	6.501	1.223	2.705	2.245	9.96	105.77	0.00828
V9	3.578	1.182	86.44	3.024	11.17	21.239	0.00603
V10	5.698	1.213	28.15	2.837	8.40	12.499	0.00709
V11	6.828	1.22	36.69	2.74	8.21	11.477	0.00766
V12	5.177	1.204	30.84	2.671	9.51	12.208	0.00694

R_s and R_{sh} values were measured by the LabVIEW setup using the conventional slope method that measures R_s and R_{sh} from the slopes of I–V curves at open circuit and short circuit conditions respectively. This conventional method, here called the 'Slope' method, usually gave higher values of R_s compared to PSO method as shown for two samples V1 and V2 in Table 3. This would be expected since the 'Slope' method assumes a single diode model to be applicable. However, R_{sh} values from the 'Slope' method matched well with those estimated from the PSO method. Parameters of two solar cell samples, V1 and V2 were also estimated using Differential Evolution (DE) algorithm [25,26] for the purpose of comparison. All the estimated parameters of samples V1 and V2 for two-diode model are tabulated in Table 3 for PSO and DE algorithms. The values of different solar cell parameters estimated by two algorithms are quite comparable, which confirms the sanctity of our results using PSO algorithm.

5.2. Three-diode model with variable R_s

5.2.1. Parameter estimation using curve-fitting

Fitting of calculated current to the measured current for different cell voltages using the three diode model with variable R_s and the PSO algorithm was carried out for the same 12 industrial samples, out of which results for two samples are shown in Fig. 6. For sample V1, MAE value obtained was 0.00645 A, which was 0.115% of I_{sc}. For sample V2, MAE value obtained was 0.0061 A, which was 0.108% of I_{sc}. Best and worst values of MAE in percentage were 0.106% of I_{sc} for V7 and 0.171% of I_{sc} for V8. I_{sc}, was approximately 5.6A for all samples.

Table 4 gives the estimated parameters using the three-diode model with variable R_s for 12 samples. We found that value of n_3 varied between 2.183 and 2.414. I_{01} and I_{02} for the three-diode model were much less compared to the corresponding I_{01} and I_{02} values for the two-diode model (Table 2).

5.2.2. R_s variation with current I

Estimated values of R_{so} and K (Table 4) showed that R_s increased with increase in load current since values of K were positive. The variation in the value of R_s (in percentage) from the open-circuit condition (current = 0) to the short-circuit condition (current = I_{sc}), for samples V1 to V5, is shown in Table 5. R_{so} represents the value of the series resistance under the open-circuit condition and R_s at I_{sc} represents the value of the series resistance under the short-circuit condition. It can be seen from the

Table 3
Comparison of estimated parameters using Slope, PSO and DE algorithms for samples V1 and V2. Samples. Slope method is the conventional method that measures R_s and R_{sh} from the slopes of the I–V cure at V_{oc} and I_{sc} respectively.

	Method	I_{01} (nA)	n_1	I_{02} (μA)	n_2	R_s (mΩ)	R_{sh} (Ω)	MAE (A)
V1	Slope					17.2	64.3	
	PSO	6.449	1.216	36.2	2.727	11.67	63.46	0.00626
	DE	8.723	1.234	51.04	2.913	11.61	63.52	0.00625
V2	Slope					19.0	15.8	
	PSO	4.311	1.195	63.32	2.794	13.29	16.183	0.00604
	DE	5.341	1.206	69.99	2.848	13.23	16.482	0.00605

Table 5 that the variation of R_s with load current, I (from I = 0 to $I = I_{sc}$), was very small, between 5 and 10% for different samples. Some researchers [29–31] have earlier worked on variation of R_s, for dark ($R_{s,dark}$) and for light conditions ($R_{s,light}$) and their variation with the load current density but contradictory findings have been reported. Aberle et al. [29] have studied variation of $R_{s,dark}$ and $R_{s,light}$ with the load current density at various light intensities for a 19% efficient 45 cm^2 area silicon solar cell and found that $R_{s,dark}$ decreases at a slow rate and $R_{s,light}$ increases at a much faster rate with the load current density. Smirnov and Mahan [30] have shown an increase in the series resistance, R_s, with the load current density on a model device with an illuminated area of 1×1 cm^2. Fong et al.

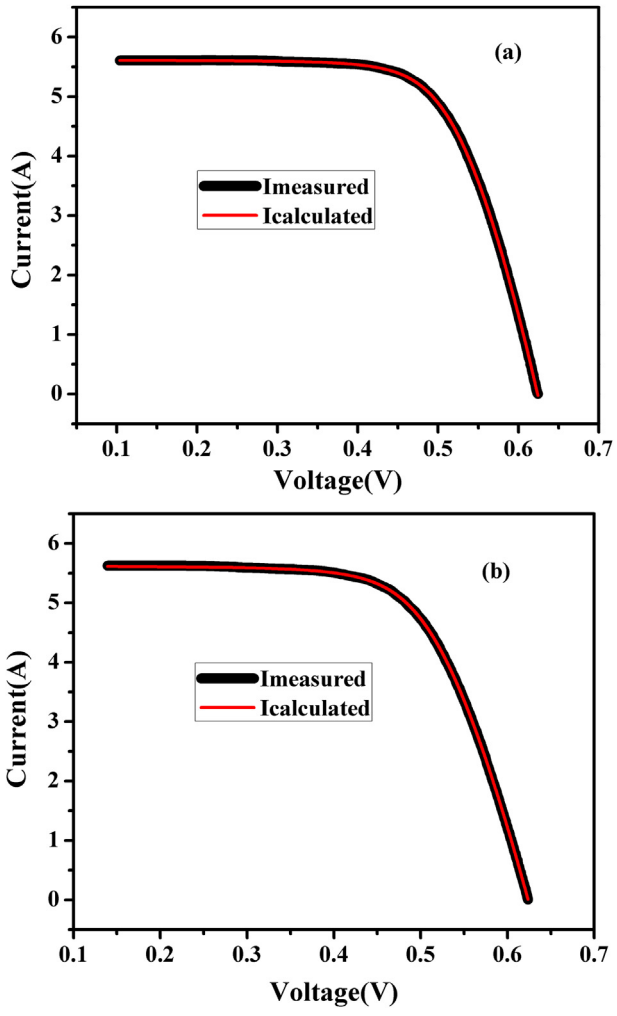

Fig. 6. I–V characteristics for (a) Sample V1 and (b) Sample V2. Calculated characteristics using the three-diode model compare well with the measured characteristics.

Table 4
Estimated parameters using the three-diode model with variable series resistance, R_s.

Samples	I_{01} (pA)	I_{02} (nA)	I_{03} (μA)	n_3	R_{so} (mΩ)	K	R_{sh} (Ω)	MAE (A)
V1	71.27	72.57	16.64	2.342	12.01	0.01838	64.419	0.00645
V2	67.91	50.83	20.68	2.333	13.75	0.00992	16.341	0.0061
V3	68.92	41.51	12.02	2.285	15.51	0.01459	36.574	0.00602
V4	68.5	26.29	7.941	2.189	12.33	0.01834	9.49	0.0064
V5	72.69	32.99	8.114	2.183	9.31	0.01745	21.012	0.00643
V6	70.32	69.57	13.3	2.362	12.69	0.01256	14.907	0.00636
V7	71.51	47.76	15.68	2.385	11.58	0.01435	15.47	0.00595
V8	61.98	77.4	6.538	2.204	10.4	0.01865	100.73	0.00952
V9	68.66	88.43	14.33	2.274	11.57	0.00995	21.128	0.00608
V10	65.16	64.46	13.43	2.345	8.92	0.01852	12.46	0.0075
V11	71.91	57.18	21.09	2.414	8.53	0.02879	12.196	0.00753
V12	69.41	79.58	8.783	2.184	9.88	0.01795	12.127	0.00684

[31] have worked on two solar cell structures, an inter-digited back contact (IBC) solar cell and an elongated solar cell and both samples have shown a decrease in $R_{s,light}$ at different rates with the load current density. Smirnov and Mahan [30] had earlier calculated the variation of R_s with load current to be as much as 200% for solar cells of area ~1×1 cm. Our results showed that in large commercial cells, this would not be true and variation of R_s with load current would be within 10%. Perhaps the increase in R_s value at high current densities due to effects like current crowding might not be much in large size industrial silicon solar cells with well-designed grid patterns.

6. Comparison of the two-diode model and the three-diode model with variable R_s

6.1. MAE values in the two models

MAE values were compared for different silicon solar cell samples for the two models. General observation is that, MAE was a little higher for the three-diode model in most cases, as compared to the two-diode model as shown in Fig. 7. In some cases, the MAE was lower for the three-diode model. A little higher values of MAE (still up to third decimal place) did not have observable effect on the fitting of the calculated curve to the measured curve (Fig. 6).

6.2. Estimated parameter values in two models

Comparison of solar cell parameters estimated using the two models is shown in Table 6 for two silicon solar cell samples, V1 and V2.

The values of I_{01} and I_{02} obtained for the 3-diode model were 2–3 orders of magnitude smaller than the corresponding values of I_{01} and I_{02} in the two-diode models. Also, for the three-diode model, I_{02} was 2–3 orders of magnitude smaller than I_{03}. In the three-diode model, n_1 was taken as 1 for the diode current contribution due to diffusion and recombination in the QNRs of bulk and emitter regions; n_2 was taken as 2 for the diode current

Table 5
Variation of R_s with current I (in %).

Sample	R_{so} (mΩ)	K	I_{sc} (A)	R_s at I_{sc} (mΩ)	Variation of R_s with I ($I = 0$ to $I = I_{sc}$) (%)
V1	12.01	0.01838	5.61	13.2484	10.31
V2	13.75	0.00992	5.628	14.5177	5.58
V3	15.51	0.01459	5.605	16.7783	8.18
V4	12.33	0.01834	5.640	13.6055	10.34
V5	9.31	0.01745	5.554	10.2122	9.69

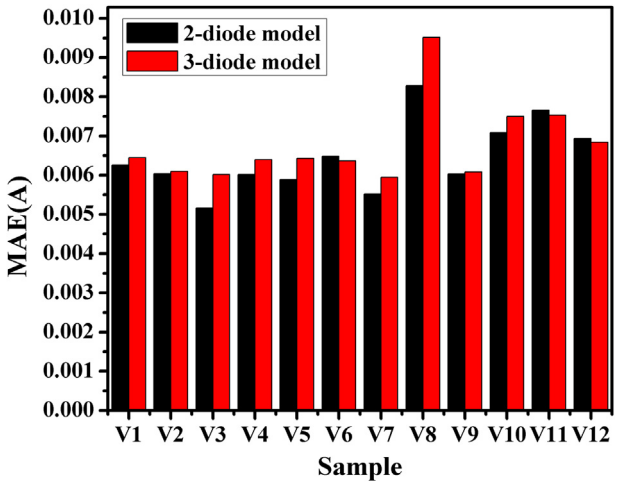

Fig. 7. Comparison of mean absolute error (MAE) values for the two different models showing that they were comparable for the two models.

contribution due to recombination in the SCRs of the p–n junction. n_3 estimated through PSO was found to be between 2 and 2.5, which contributed to the diode current due to recombination in the defect sites. We also found that the diode current due to bulk and emitter recombination was getting masked and the I_{d1} obtained from the two-diode model was due to the mixed effect of bulk and emitter recombination and space charge recombination. Therefore, the three-diode model clearly separated the three contributions to the diode current and would be, therefore, a better model to describe the I–V characteristics of the large size industrial silicon solar cells.

7. Conclusions

A new equivalent circuit model using three diodes has been proposed in this work, to model industrial crystalline silicon solar cells of large area. This would be a better model to describe the I–V characteristics of large size solar cells as compared to the one-diode or two-diode models existing in the literature. Series resistance of these solar cell samples has been found to increase with increase in load current from open-circuit to short-circuit conditions. This variation was found to be between 5 and 10% for these bigger size industrial solar cells.

PSO algorithm has been applied to estimate the solar cell parameters of the two-diode model and the proposed three-diode model from the illuminated I–V characteristics measured using a solar simulator. Parameters were estimated using an iterative PSO approach from the I–V characteristics. Although PSO is a random approach, but in this work, we have shown that the multiple PSO runs gave consistent results. PSO was, therefore, found to be a good method for precise estimation of solar cell parameters, with Mean Absolute Error not exceeding 0.18% of I_{sc}, for any sample.

Finally, the proposed three-diode model has been compared with the two-diode model. The estimated values of n_1 (>1) and n_2 (>2) in the two-diode model for the industrial samples were not found to be in conformity with the theoretical values ($n_1 = 1$ and $n_2 = 2$). The three-diode model with $n_1 = 1$, $n_2 = 2$ and estimated values of n_3 (>2) was found to be a better model to clearly separate the different diode current components in industrial solar cell samples.

Table 6
Comparison of two models for samples V1 and V2.

Samples	V1		V2	
Models	2-diode	3-diode, variable R_s	2-diode	3-diode, variable R_s
I_{01} (A)	6.45E-09	7.13E-11	4.31E-09	6.79E-11
n_1	1.216	1	1.195	1
I_{02} (A)	3.62E-05	7.26E-08	6.33E-05	5.08E-08
n_2	2.727	2	2.794	2
I_{03} (A)	–	1.66E-05	–	2.07E-05
n_3	–	2.342	–	2.333
R_s (mΩ)	11.7	12.0 (R_{so})	13.3	13.8 (R_{so})
R_{sh} (Ω)	63.46	64.419	16.183	16.341
K	–	0.0184	–	0.0099
MAE (A)	0.00626	0.00645	0.00604	0.0061

Acknowledgement

We like to acknowledge the NWP-55 Grant from CSIR, India, as some measurements were carried using the facility created under this grant (TAPSUN initiative of CSIR).

References

[1] Tsai Huan-Liang. Insolation-oriented model of photovoltaic module using Matlab/simulink. Sol Energy 2010;84(7):1318–26.
[2] Saloux Etienne, Teyssedou Alberto, Sorin Mikhaïl. Explicit model of photovoltaic panels to determine voltages and currents at the maximum power point. Sol Energy 2011;85(5):713–22.
[3] Ishaque Kashif, Salam Zainal, Taheri Hamed. Simple, fast and accurate two-diode model for photovoltaic modules. Sol Energy Mater Sol Cells 2011;95(2):586–94.
[4] Sheriff MA, Babagana B, Maina BT. A study of silicon solar cells and modules using PSPICE. World J Appl Sci Technol 2011;3(1):124–30.
[5] Nema RK, Nema Savita, Agnihotri Gayatri. Computer simulation based study of photovoltaic cells/modules and their experimental verification. Int J Recent Trends Eng 2009;1(3):151–6.
[6] Ishaque Kashif, Salam Zainal, Taheri Hamed, Syafaruddin. Modeling and simulation of photovoltaic (PV) system during partial shading based on a two-diode model. Simul Model Pract Theory 2011;19(7):1613–26.
[7] Patel H, Agarwal V. Matlab-based modeling to study the effects of partial shading on PV array characteristics. IEEE Trans Energy Convers 2008;23(1):302–10.
[8] Ishaque Kashif, Salam Zainal, Syafaruddin. A comprehensive MATLAB Simulink PV system simulator with partial shading capability based on two-diode model. Sol Energy 2011;85(9):2217–27.
[9] Bouzidi K, Chegaar M, Bouhemadou A. Solar cells parameters evaluation considering the series and shunt resistance. Sol Energy Mater Sol Cells 2007;91(18):1647–51.
[10] Bouzidia K, Chegaara M, Aillerieb M. Solar cells parameters evaluation from dark I-V characteristics. Energy Procedia 2012;18:1601–10.
[11] Chegaar M, Ouennoughi Z, Guechi F. Extracting dc parameters of solar cells under illumination. Vacuum 2004;75(4):367–72.
[12] Haouari-Merbah M, Belhamel M, Tobías I, Ruiz JM. Extraction and analysis of solar cell parameters from the illuminated current–voltage curve. Sol Energy Mater Sol Cells 2005;87(1–4):225–33.
[13] Tivanov M, Patryn A, Drozdov N, Fedotov A, Mazanik A. Determination of solar cell parameters from its current–voltage and spectral characteristics. Sol Energy Mater Sol Cells 2005;87(1–4):457–65.
[14] Ortiz-Conde A, Garcia Sanchez FJ, Muci J. New method to extract the model parameters of solar cells from the explicit analytic solutions of their illuminated I–V characteristics. Sol Energy Mater Sol Cells 2006;90(3):352–61.
[15] Jervase Joseph A, Bourdoucen Hadj, Al-Lawati Ali. Solar cell parameter extraction using genetic algorithms. Meas Sci Technol 2001;12:1922–5.
[16] AlRashidi MR, AlHajri MF, El-Naggar KM, Al-Othman AK. A new estimation approach for determining the I–V characteristics of solar cells. Sol Energy 2011;85(7):1543–50.
[17] AlHajri MF, El-Naggar KM, AlRashidi MR, Al-Othman AK. Optimal extraction of solar cell parameters using pattern search. Renew Energy 2012;44:238–45.
[18] AlRashidi MR, El-Naggar KM, AlHajri MF. Heuristic approach for estimating the solar cell parameters. In: Proceedings of the 5th WSEAS congress on applied computing conference, and proceedings of the 1st international conference on biologically inspired computation (BICA'12); 2012. p. 80–3.
[19] Phuangpornpitak N, Prommee W, Tia S, Phuangpornpitak W. A study of particle swarm technique for renewable energy power systems. In: Proceedings of the international conference on energy and sustainable development: issues and strategies (ESD), 2–4; June 2010.
[20] Kongnama C, Nuchprayoon S. A particle swarm optimization for wind energy control problem. Renew Energy 2010;35(11):2431–8.
[21] Qin Hengsi, Kimball JW. Parameter determination of photovoltaic cells from field testing data using particle swarm optimization. In: Power and Energy conference at Illinois (PECI), 2011 IEEE; 25-26 Feb 2011. p. 1–4.

[22] Sandrolini L, Artioli M, Reggiani U. Numerical method for the extraction of photovoltaic module double-diode model parameters through cluster analysis. Appl Energy 2010;87(2):442–51.
[23] Shahzad Farrukh, Rauf Baig A, Masood Sohail, Kamran Muhammad, Naveed Nawazish. Opposition-based particle swarm optimization with velocity clamping (OVCPSO). Adv Intelligent Soft Comput 2009;116:339–48.
[24] Engelbrecht Andries P. Computational intelligence: an Introduction. 2nd ed. Wiley; 2007.
[25] Jiang Lian Lian, Maskell Douglas L, Patra Jagdish C. Parameter estimation of solar cells and modules using an improved adaptive differential evolution algorithm. Appl Energy 2013;112:185–93.
[26] Ishaque Kashif, Salam Zainal, Mekhilef Saad, Shamsudin Amir. Parameter extraction of solar photovoltaic modules using penalty-based differential evolution. Appl Energy 2012;99:297–308.
[27] Steingrube Silke, Breitenstein Otwin, Ramspeck Klaus, Glunz Stefan, Schenk Andreas, Altermatt Pietro P. Explanation of commonly observed shunt currents in c-Si solar cells by means of recombination statistics beyond the Shockley-Read-Hall approximation. J Appl Phys 2011;110(1). 014515-1–014515-10.
[28] Nishioka Kensuke, Sakitani Nobuhiro, Uraoka Yukiharu, Fuyuki Takashi. Analysis of multicrystalline silicon solar cells by modified 3-diode equivalent circuit model taking leakage current through periphery into consideration. Sol Energy Mater Sol Cells 2007;91(13):1222–7.
[29] Aberle AG, Wenham SR, Green MA. A new method for accurate measurements of the lumped series resistance of solar cells. In: Photovoltaic Specialists conference. Conference record of the twenty third IEEE, 10-14 May 1993; 1993. p. 133–9.
[30] Smirnov Georgy M, Mahan John E. Distributed series resistance in photovoltaic devices; intensity and loading effects. Solid-State Electron 1980;23(10):1055–8.
[31] Chern Fong Kean, McIntosh KR, Blakers AW, Franklin ET. Series resistance as a function of current and its application in solar cell analysis. In: 37th IEEE photovoltaic specialists conference, photovoltaic Specialists conference (PVSC); 19-24 June 2011. p. 002257–61.